Silica-Based Planar Lightwave Circuits: Passive and Thermally Active Devices

Tetsuo Miya, *Member, IEEE*

Invited Paper

***Abstract*—Silica-based planar lightwave circuits (PLC's) are playing key roles in both optical dense wavelength-division multiplexing networks and optical access networks. This paper provides an outline of PLC technology focusing on passive devices such as arrayed waveguide grating multiplexers.**

***Index Terms*—Arrayed-waveguide grating multiplexers, dispersion equalizers, hybrid integrated circuits, integrated optics, optical switches, optical waveguide components, planar waveguides, silica-based waveguide, waveguide filters, waveguide switches, wavelength-division multiplexing.**

I. Introduction

THE DEMAND for greater bandwidth in networks is increasing at a tremendous rate owing to the rapid spread of the Internet and multimedia communications. Optical networks and communication systems with enormous transmission capacity and bandwidth are being used to achieve a quantum leap in communication bandwidth. Wavelength-division multiplexing (WDM) [1], where different channels are transmitted at different wavelengths, can be used to exploit the enormous bandwidth of optical networks and communication systems. Optical access networks for fiber-to-the-home (FTTH) [2], [3] have been installed in Japan to enlarge the network service capacity and to increase its flexibility. A number of studies are under way with a view to realizing optical communication networks with larger capacity and more flexibility [4].

To realize these network communication system demands, we must develop optical devices with appropriate characteristics that are inexpensive, easy to handle, and highly reliable. Planar lightwave circuits (PLC's), in which fiber-matched silica-based waveguides are integrated, show excellent promise and can provide various key practical devices for such optical networks.

Owing to their excellent performance, a number of PLC devices are already being used in commercial optical network systems, and others will be employed in future photonic networks. For example, $1\times N$ optical splitters are used in optical passive double star systems in access networks. Optical network units [5], [6] which act as O/E, E/O converters, are used in the FTTH network system. Arrayed waveguide grating multi/demultiplexers (AWG's) are playing a key role in dense WDM network systems. PLC devices include wavelength $N \times N$ multi/demultiplexers, optical add/drop or cross-connect switches, multiwavelength light sources for WDM transport networks, and programmable filters [7], [8] for high-speed transmission systems.

This paper offers a brief description of PLC devices focusing on passive devices such as $1\times N$ splitters, AWG's, thermooptic switches, and dispersion equalizers with an emphasis on NTT achievements. Hybrid PLC devices will be described in another paper in this issue.

II. Features of PLC Devices

PLC devices have numerous advantages as regards their use in optical fiber communication systems. As explained in the next section, PLC technology [9] is a combination of optical fiber fabrication technology and large-scale integrated circuit (LSI) patterning technology, which provides low-loss characteristics and high productivity. PLC devices match single-mode optical fibers well from the viewpoint of materials and optical characteristics. Since the waveguide material is silica glass, PLC devices have high reliability. PLC technology can be used to realize passive optical devices such as filters, switches, and slope dispersion equalizers. These optical devices are transparent in terms of transmission protocol, transmission bit rate, and loss, thus simplifying optical network system design. Furthermore, the use of hybridization techniques [10]–[13], means that semiconductor chips as laser diodes and photo detectors can be mounted on PLC platforms to realize more functional hybrid PLC devices [14]–[19].

III. Fabrication

Silica-based PLC's are fabricated on silicon substrates or quartz substrates using a series of techniques comprising waveguide-layer deposition, waveguide formation, packaging, and optical circuit design. A schematic of the waveguide fabrication process is shown in Fig. 1. The first step in the process is formation of the waveguide-layer. The layer can be formed using several techniques, such as flame hydrolysis deposition (FHD) and chemical vapor deposition (CVD). Among them we usually use the FHD technique [9] in NTT. In the FHD process, fine glass particles or soot chemically produced in an oxy-hydrogen flame is deposited on Si or quartz substrates. After deposition, the substrates are then heated in

Manuscript received October 21, 1999; revised November 19, 1999.

The author is with NTT Photonics Laboratories, Tokai, Ibaraki 319-1193, Japan (e-mail: miya@iba.iecl.ntt.co.jp).

Publisher Item Identifier S 1077-260X(00)01562-8.

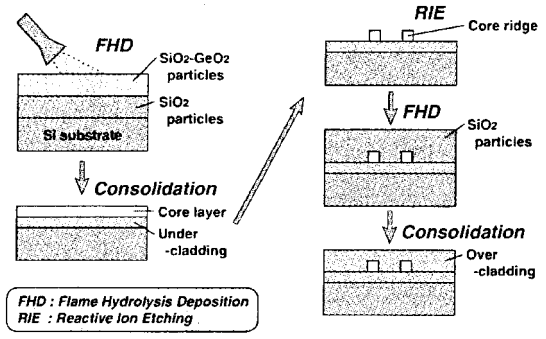

Fig. 1. Schematic of PLC fabrication process.

an electric furnace to about 1000 °C, and the glass particle layers become transparent glass layers. The FHD technique, the soot process, and the consolidation process constitute an improved version of vapor-phase axial deposition method [20], one of the widely used optical fiber fabrication methods. One of the advantages of FHD is that it can be used to form low-loss transparent layers and glass layers with a wide range of thickness—from several to tens of micrometers, and, in a special case, on the order of 100 μm. The waveguide layer is patterned by reactive ion etching (RIE), which is a technique widely used for patterning LSI's. It should be noted that owing to the well-defined waveguide structure provided by RIE, the characteristics of simulated and fabricated circuits agree well, even when the circuits are complicated. Improved fabrication techniques have led to the realization of a low loss of 0.017 dB/cm in a 10-m-long waveguide withΔ equal to 0.45% [21].

The characteristics of four typical silica-based waveguides are shown in Table I. Both the propagation loss and the bending loss depend on the Δ value, and they are in the tradeoff relationship with each other in terms of Δ value.

1) The propagation loss (sum of the scattering loss and the absorption loss) in the waveguide increases with the increasing dopant concentration or Δ value.
2) On the other hand, the bending loss becomes lower with the increasing Δ value.

We can make full use of these characteristics of waveguides to realize a variety of PLC devices.

Since low Δ waveguides have almost the same spot size as 1.3-μm zero-disperison single-mode optical fibers (SMF's), they are used in optical devices whose insertion loss must be very low. By contrast, devices such as 8×8 matrix thermooptic switches with complicated circuits are fabricated using high or super-high Δ waveguides, making use of their small bending loss.

IV. Splitter and WINC

Optical couplers/splitters [22]–[30] are indispensable for distributing optical signals from a trunk line to branch lines in optical subscriber networks. They play a key role in the passive double-star based FTTH system. The splitter family includes not only 1×8 splitters but also 1×16, 1×32, 2×8, 2×16, and 2×32 splitters. Studies have recently been undertaken to integrate optical circuits more densely on a wafer in order to reduce the cost and the space required per unit circuit.

TABLE I
Waveguide Characteristics

	Low-Δ	Middle-Δ	High-Δ	Super High-Δ
Refractive Index Difference Δ (%)	0.25	0.45	0.75	1.5
Core Size (μm)	8 x 8	7 x 7	6 x 6	4.5 x 4.5
Propagation Loss (dB/cm)	< 0.01	0.02	0.04	0.07
Fiber Coupling Loss (dB/point)	< 0.1	0.1	0.5	2.0 (SMF) 0.4 (DSF)
Minimum Bending Radius (mm)	25	10	5	2
Application Field	Small-Scale PLC	Medium-Scale PLC	Large-Scale PLC	Very Large-Scale & High-Density PLC

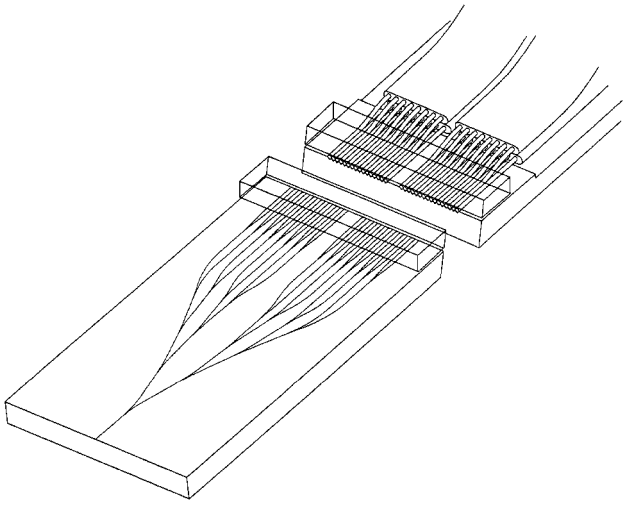

Fig. 2. A schematic of $1\times$ 32 splitters and a dense 32 fiber array block.

As a result, for example, the chip size of highly compact 1×32 splitters has been reduced to $6\times$ 24 mm ^{2} by using a 127-μm pitch fiber array and 0.4%-Δ waveguides with a 15-mm bending radius [22]. This is about 1/4 the size of conventional 1×32 splitters. Fig. 2 shows a schematic of 1×32 splitters and a dense 32 fiber array block before bonding.

Detailed studies [23]–[26] have been made of splitter reliability because splitters are fundamental PLC devices. Fig. 3 shows the results [23] of a damp heat test based on Bellcore specifications. The loss variations are small and satisfy the specifications. The splitters also passed all other reliability tests as shown in Table II.

The bonding and packaging techniques developed for the splitters have been adopted for other PLC devices such as AWG's and have also been confirmed to offer long term reliability.

Wavelength-insensitive couplers (WINC's) [27], [28] are optical couplers whose coupling ratios do not depend on wavelength. As optical devices that employ directional couplers are generally wavelength dependent, this makes WINC's particularly desirable in terms of network system design. They are installed in optical network monitoring system in optical networks called AURORA [29] in which 1.55 μm is the transmission signal wavelength and 1.65 μm is the monitoring wavelength.

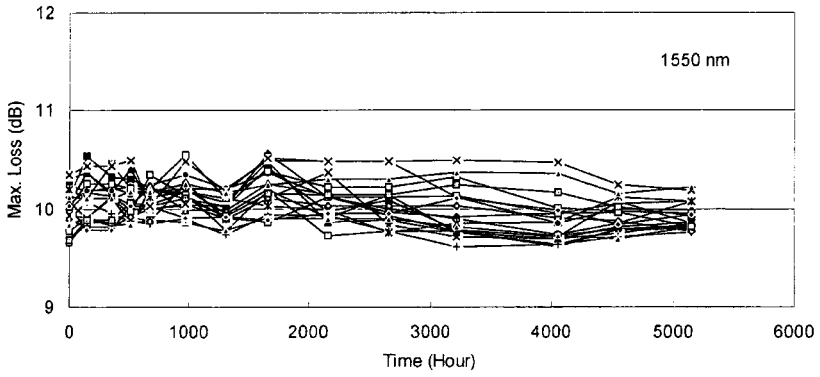

Fig. 3. Result of damp heat tests (75 °C, 90%RH).

TABLE II
AVERAGE LOSS CHANGES AT 1.55 μm AFTER RELIABILITY TESTS OF 1× 8 SPLITTER MODULES

No.	Test	Duration	Samples	Loss Change (dB)
1	Damp heat (75℃, 90%RH)	5156 hours	19	- 0.12
2	High temperature (85℃, < 90%RH)	5090 hours	11	- 0.16
3	Temperature cycle (-40 ~ 75℃)	377 cycles	11	0.03
4	Heat shock (ΔT = 100℃)	20 cycles	11	0.01
5	Water immersion (43℃)	168 hours	11	- 0.01
6	Salt spray (35℃, 5%)	168 hours	11	0.02
7	Vibration (10 ~ 2000 Hz)	3 direction 12 cycles	11	- 0.01

V. ARRAYED WAVEGUIDE GRATING

An$N \times N$ AWG multiplexer has excellent potential for use in optical WDM networks since it is capable of simultaneously processing N^2 optical channels at N different wavelengths as a result of multibeam interference [31]–[33]. As shown in Fig. 4, it consists of two concave slab waveguides and some hundreds of waveguides, which are arrayed between them with a constant optical path differenceΔL between each adjacent pair. This constant optical path difference causes wavelength dependent tilting in the second slab region. The input light is radiated to the first slab waveguide and then excites the arrayed waveguides. After traveling through the arrayed waveguides, the light beam interferes constructively at one focal point in the second slab. The location of the focal point depends on the signal wavelength λ [34], because the relative phase delay in each arrayed waveguide is given by $2\pi\Delta L/\lambda$. Thus it functions as a grating.

The dispersion of the focal position x versus the wavelengthλ is expressed as

$$dx/d\lambda = fmn_g/n_s dn_c \quad \text{where } m = n_c\Delta L/\lambda_0.$$

Here, f is the focal length of the slab waveguide, n_s and n_c are the effective indexes in the slab waveguide and the channel waveguide, respectively, n_g, is the group index in the channel waveguide, d is the arrayed waveguide pitch, m is the diffraction order, and λ_0 is the center wavelength. By designing the λL value, it is possible to achieve AWG's with a desired channel spacing and channel number. A thin polyimide half-wavelength film is inserted into the midpoint of the arrayed waveguides to eliminate polarization dependence [35]. Another approach to eliminating waveguide polarization is the use of a dopant-rich silica-based glass whose thermal expansion coefficient is adjusted to that of the Si substrate [36].

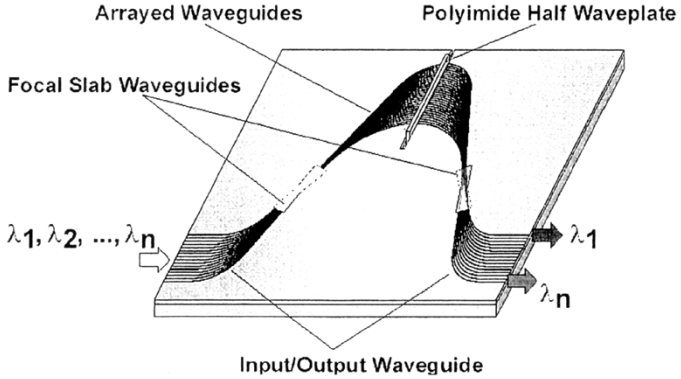

Fig. 4. Schematic configuration of $N \times N$ arrayed-waveguide grating multiplexer.

Table III shows the experimental characteristics of a series of AWG's. One of the advantages of the AWG is the flexibility of its channel number and channel spacing and, as a result, various kinds of AWG's can be fabricated in a similar manner. Channel numbers range from eight with a 15-nm channel spacing to 128 with a 25-GHz (15 nm) channel spacing. The demultiplexing characteristics of a 25-GHz channel spacing 128-channel AWG [37] are shown in Fig. 5. The crosstalk to the neighboring channels is less than −16 dB, and the on-chip loss ranges from 3.5 dB

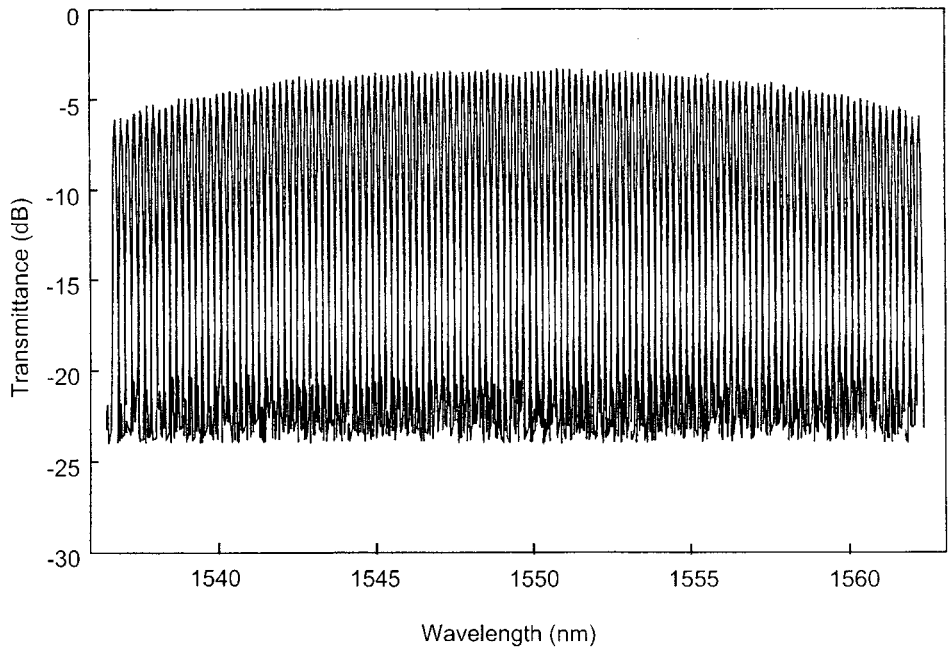

Fig. 5. Demultiplexing characteristics of 128-channel, 25-GHz spacing AWG.

TABLE III
EXPERIMENTAL PERFORMANCE OF FABRICATED AWG'S

Parameters	Experimental Results					
Channel Spacing $\Delta\lambda$	15 nm	0.8 nm (100 GHz)			0.2 nm (25 GHz)	Unequal (0.8/0.48 nm)
Number of Channels N	8	16	32	64	128	16
Path Difference ΔL	12.8 μm	63.2 μm	63.0 μm	30.9 μm	63.0 μm	79.21 μm
Focal Length F	2.38 mm	9.01 mm	11.35 mm	18.50 mm	36.30 mm	14.42 mm
Diffraction Order m	12	59	59	29	59	74
On-Chip Loss	2.4 dB	6.4 dB	2.1 dB	2.8 dB	3.5 dB	2.8 dB
3-dB Passband $FWHM$ ($FWHM/\Delta\lambda$)	6.3 nm (42 %)	78 GHz (78 %)	40 GHz (40 %)	44 GHz (44 %)	11 GHz (44 %)	30.2 GHz
Channel Crosstalk	< -28 dB	< -32 dB	< -28 dB	< -29 dB	< -16 dB	< -25 dB

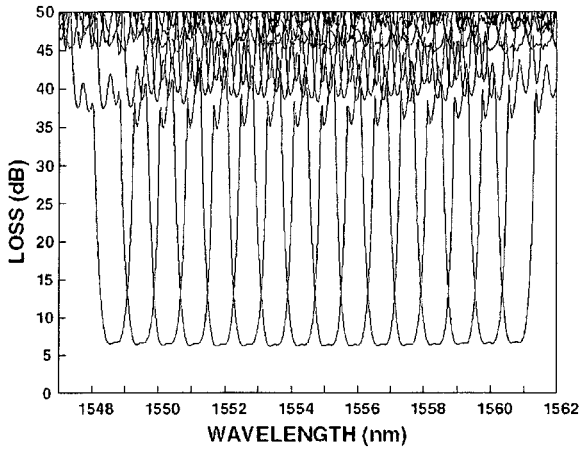

Fig. 6. Transmission spectra of flat-passband, low-crosstalk AWG.

for the central output ports to 5.9 dB for the peripheral output ports. The crosstalk in the AWG's is mainly caused by the phase errors in the arrayed waveguides. By refining the core fabrication process, a very low crosstalk of about −50 dB has been successfully achieved.

The channel number is an important parameter as regards the degree of multiplexing and expansion of application area. The largest AWG channel number in Table III is 128. A further increase in AWG channel number will be reported in the near future.

In practical use, flat and wide passband characteristics are required in order to suppress the loss deviation die to the wavelength fluctuation of the light sources and AWG's. To achieve such characteristics, a rectangular optical field has to be generated at a connection point between slab and input or output waveguides. Methods already proposed include the Y-branch [38], sinc-functional field [39], multimode interference [40], two focal-point method [41], double-pass method [42] and parabolic taper method [43]. A typical example of a flat passband AWG [43] fabricated by the parabolic taper method is shown in Fig. 6. The 1-, 3-, and 20-dB bandwidths are 98, 124, and 196 GHz, respectively, for a 200-GHz channel spacing. The bandwidth of this AWG is about twice that of a conventional one and meets the system needs. The crosstalk to the neighboring ports was < -27 dB, and the chip insertion loss was 6.1 dB.

Temperature-independent devices are very attractive from the practical point of view. Conventional AWG's have a temperature dependence of about 0.013 nm/°C, which is caused by the thermally induced refractive index change in silica glass waveguides. In practical use, thermooptic coolers or heaters are used to compensate for the temperature dependence of the waveguides and stabilize the AWG performance. An athermal AWG [44] with negligible temperature sensitivity has been reported, in which the negative temperature dependence of the silicone adhesive resin in the narrow grooves in the optical waveguides cancels out that of the waveguides. The configuration is shown in Fig. 7. The refractive index of silicone has a negative thermal

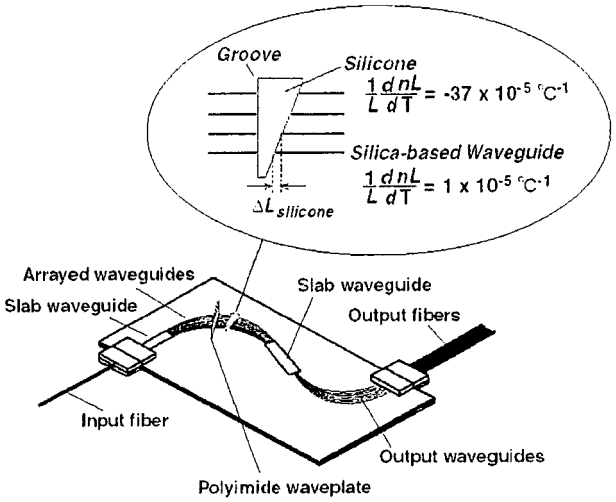

Fig. 7. Schematic configuration of athermal AWG.

coefficient, and its absolute value is one order larger than that of silica-based waveguides. The groove is designed to satisfy the following athermal condition:

$$d(n_{\mathrm{wg}} \cdot \Delta L_{\mathrm{wg}})/dT + d(n_{\mathrm{silicone}} \cdot \Delta l_{\mathrm{silicone}})/dT = 0$$

where T is the AWG chip temperature, n_{wg} and n_{silicone} are the refractive indexes of the silica-based waveguides, and silicone, respectively, andΔL_{wg} and$\Delta l_{\mathrm{silicone}}$ are the path differences of the arrayed waveguides and the silicone between adjacent arrayed waveguides, respectively.

The temperature dependence of the wavelength responses is shown in Fig. 8 for conventional and athermal 1×8 AWG's with a channel spacing of 100 GHz. The temperature-dependent wavelength drift was suppressed from 0.95 to 0.05 nm in a temperature range of 0 °C–85 °C. The excess loss caused by the groove was estimated to be 2 dB. High thermal reliability was confirmed with a loss change of 0.2 dB in a heat cycle test from −40 °C to 85 °C, and the wavelength change was only 0.02 nm in a 5000 h, 75 °C, and 90% relative humidity test. These results show that the athermal AWG requires no thermal control for practical use.

VI. Thermooptic Switch [45]–[51]

Optical switching systems are needed for the construction of such optical WDM systems as crossconnect systems and add/drop systems. The space division matrix switch is a key device for these systems because it can switch optical signals directly without signal conversion and analog and digital signals can coexist in the same system. The basic unit of the space division matrix switch is the Mach–Zehnder interferometer (MZI). It consists of two 3-dB directional couplers and two waveguide arms between them. One of the arms is equipped with a thin-film heater to control the phase difference between the two arms and thus switch the paths. The unit is usually designed to be in the cross state when no power is applied to the heater. It can be switched to the bar state by supplying power to the heater. The switching time is about 2 ms, which is acceptable for switching applications in WDM systems.

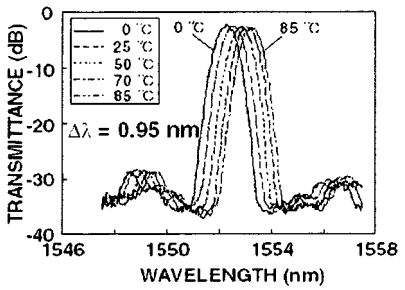

(a)

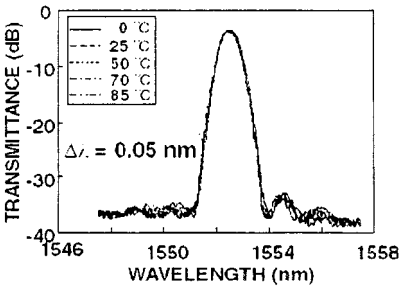

(b)

Fig. 8. Temperature-dependent transmission spectra. (a) Conventional AWG multiplexer. (b) Athermal AWG multiplexer.

$N \times N$ strictly nonblocking matrix switches $(N = 4, 8, 16)$ [45]–[50] have been fabricated using silica-based PLC's. The configurations of the switching unit and the $N \times N$ matrix switch are shown in Fig. 9. A double-gate switching unit is used to improve the extinction ratio as shown in Fig. 9(a). The unit is composed of two asymmetrical MZI's with thermooptic (TO) phase shifters and an intersection. In this configuration, the leaked output power is greatly reduced since the unwanted light power from the first MZI is blocked by the second MZI and led to the idle output port. The idle output ports are terminated within the wafer with very low reflection. Therefore, theoretically this unit can obtain double the extinction ratio of a single MZI unit. Fig. 9(b) shows the logical arrangement of an $N \times N$ matrix switch with a path-independent insertion loss arrangement [49]. This is useful for reducing the insertion loss because the total waveguide length is shorter than that in a conventional crossbar matrix switch. The average insertion loss of 6.6 dB and the average extinction ratio of 55 dB have been achieved for 16 $\times$ 16 matrix switch [48]. The electric power for operating this switching unit was about 1.1 W.

VII. Add–Drop Multi/Demultiplexer [52]–[55]

AWG's integrated with other circuits have been proposed with a view to developing new functional devices. Optical add/drop multiplexers (ADM's) incorporating AWG's and space division switches have been reported [52]. Fig. 10 shows a 16–channel optical add/drop multiplexer consisting of four AWG's with intersecting slab regions and 16 2 $\times$ 2 TO switches. These four AWG's have the same wavelength response and channel spacing of 100 GHz. Multiplexed signals are demultiplexed by AWG_1, and then 16 signals are introduced into the double-gate TO switches. When a TO switch is in the off state, a signal demultiplexed by AWG_1 passes across the TO switch and is multiplexed again by AWG_3. In contrast, when

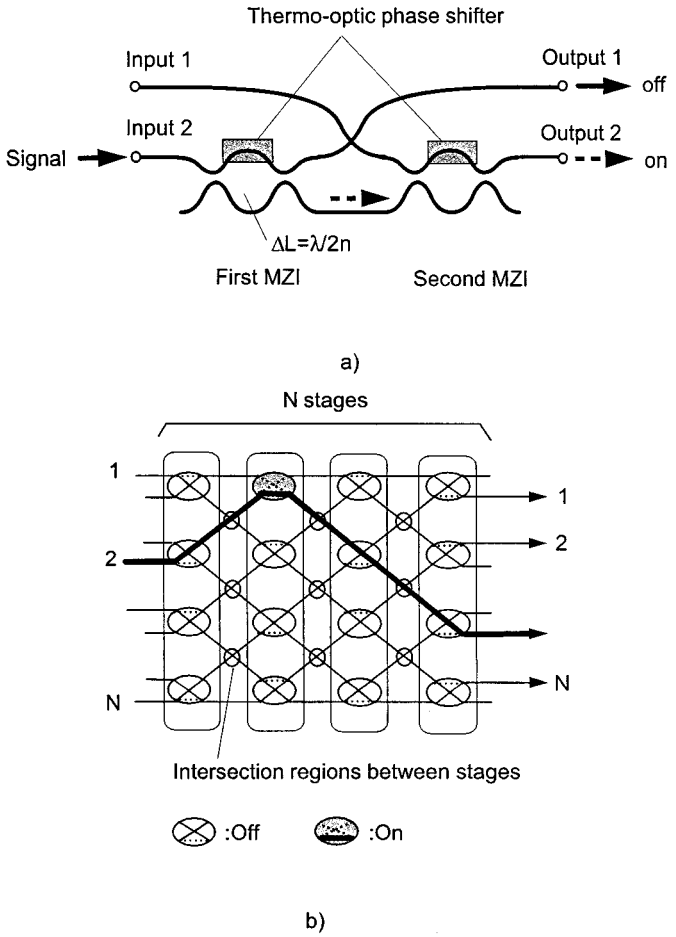

Fig. 9. Configuration of $N \times N$ matrix switch. (a) Schematic configuration of double-gate switching unit. (b) Logical arrangement of matrix switch.

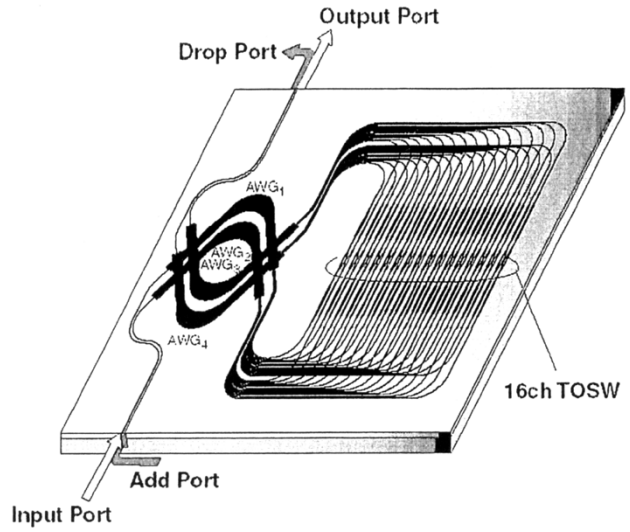

Fig. 10. Schematic configuration of 16-channel optical ADM with double-gate TO switches.

a TO switch is in the on state, a demultiplexed signal passes through the TO switch and is multiplexed again by AWG_4. Therefore, a signal at any given wavelength can be led to the drop port by operating the corresponding switch. A signal with the same wavelength as the dropped signal can be added to the

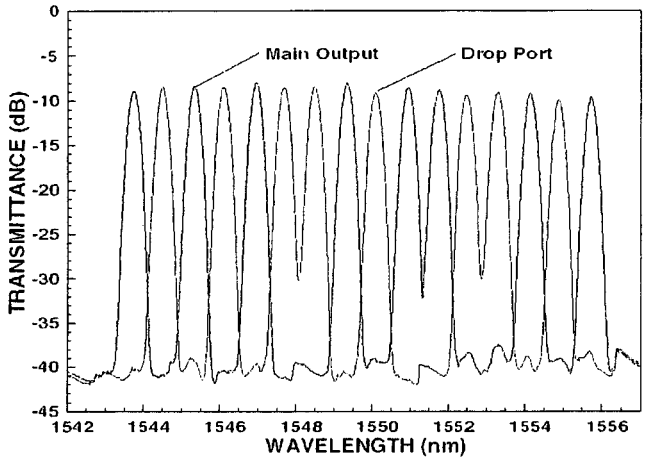

Fig. 11. Transmission spectra from main input port to main output port when TO switches $\mathrm{SW}_2, \mathrm{SW}_4, \mathrm{SW}_6, \mathrm{SW}_7, \mathrm{SW}_9, \mathrm{SW}_{12}, \mathrm{SW}_{13},$ and SW_{15} are on.

output port when it is coupled into the add port. Fig. 11 shows the transmission spectrum characteristics from the input port to the output and drop ports when eight TO switches are turned on. The corresponding wavelength signals are led to the drop port. The on–off crosstalk is less than -28.4 dB with insertion losses of 8–10 dB. The crosstalk level here is determined by the crosstalk of the AWG's because the signals pass through AWG_3 and AWG_4.

The optical ADM is a promising component for optical WDM ring networks because it can transport all signals to the following stages with no inherent power losses, and it is transparent as regards signal format and bit rate.

VIII. Dispersion Slope Equalizer

The transmission of optical signals at a high bit rate over very long distances is the goal of optical communication. The transmission distance in optical fiber communication systems has been greatly increased by the development of erbium-doped fiber amplifiers. And in optical fiber communication systems in which dispersion-shifted-fibers (DSF's) are used, the first-order chromatic dispersion has already been compensated for in the 1.55-μm wavelength region. High-bit-rate transmission of 10 and 40 Gb/s has already been successfully realized. As a result, the main factor limiting the transmission distance for optical signals with higher bit rate of, for example, multigigabit data rates in the 1.55-μm wavelength region is now the second-order chromatic dispersion in the optical fiber.

The basic configuration of a dispersion slope equalizer [56] is shown in Fig. 12. It consists of nine symmetrical MZI's interleaved with eight asymmetrical MZI's on a PLC. Thermooptic phase shifters are used for precise control of the phase-shift parameters.

Fig. 13 shows the measured relative power transmittance and relative delay time of the dispersion slope equalizer versus frequency when the free spectral range (FSR) was 200 GHz. The delay characteristics were obtained by measuring the optical phase retardation at each frequency [46]. The measured delay time can be approximated by a quadratic function with respect to the frequency. Figs. 13 and 14 show the relative delay time for a 300-km DSF without and with the equalizer. It is clear from

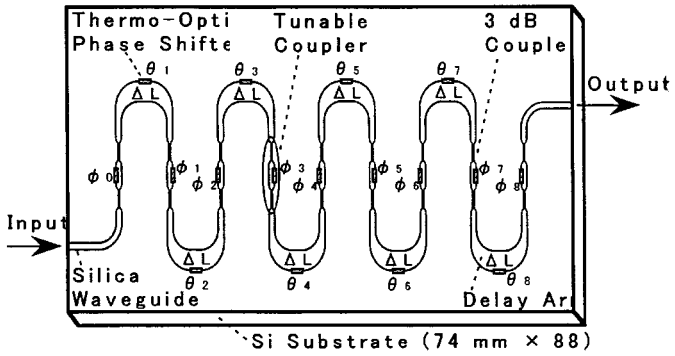

Fig. 12. Basic configuration of a dispersion slope equalizer.

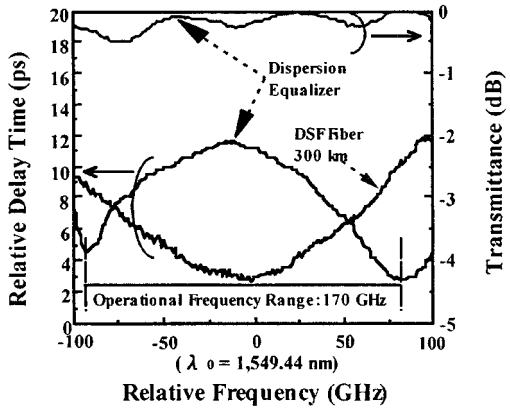

Fig. 13. Measured characteristics of a dispersion slope equalizer and a 300-km DSF.

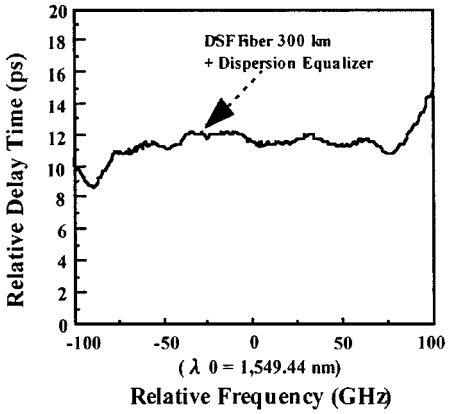

Fig. 14. Characteristic of the dispersion slope equalized 300-km DSF.

these figures that the positive dispersion slope of the DSF is almost completely compensated for by the equalizer.

IX. Conclusion

I have reviewed the recent progress on PLC's achieved in our laboratories with emphasis placed on passive devices and their application to WDM systems. We are at work to improve the characteristics of our highly reliable PLC technology and develop a variety of new functions.

Many new PLC devices have already been realized through the use of hybridization technology whereby active devices such as semiconductor laser diode chips and semiconductor optical amplifiers can be mounted on PLC platforms. Continued improvements in PLC technology, whose advantages are transparency, flexibility, and extensibility, will contribute to the development of not only optical subscriber networks but also future photonic networks.

Acknowledgment

The author would like to thank Dr. M. Kawachi and Dr. H. Yoshimura for their valuable discussions. He also thanks all the members of NTT Photonic Laboratories for their contributions to this work.

References

[1] H. Toba, K. Oda, K. Nakanishi, N. Shibata, K. Nosu, N. Takato, and M. Fukuda, "A 100-ch optical WDM transmission/distribution at 622 Mbits/s over 50 km," *J. Lightwave Technol.*, vol. 8, pp. 1396–1401, Sept. 1990.

[2] T. Miki, "Fiber-optic subscriber networks and system development," *IEICE Trans.*, vol. E74, pp. 93–100, 1991.

[3] J. Yoshida, M. Kawachi, T. Sugie, M. Horiguchi, Y. Iyaya, and M. Fududa, "Strategy for developing low-cost optical modules for the ONU of optical subscriber systems," in *Proc. IEEE Int. Workshop Access Networks*, Nuremberg, Germany, 1995. paper 61.

[4] M. Koga, Y. Hamazumi, A. Watanabe, S. Okamoto, H. Obara, K. Sato, M. Okuno, and S. Suzuki, "Design and performance of an optical path cross-connect system based on wavelength path connect," *J. Lightwave Technol.*, vol. 14, pp. 1106–1119, 1996.

[5] N. Uchida, Y. Yamada, Y. Hibino, Y. Suzuki, and N. Ishihara, "Low-cost hybrid WDM module consisting of a spot-size converted laser diode and a waveguide photodiode on a PLC platform for access network systems," *IEICE Trans. Electron.*, vol. E 80-C, pp. 88–97, 1997.

[6] Y. Yamada, S. Suzuki, K. Moriwaki, Y. Hibino, Y. Tohmori, Y. Akatsu, Y. Nakasuga, T. Hashimoto, H. Terui, M. Yanagisawa, Y. Inoue, Y. Akahori, and R. Nagase, "Application of planar lightwave circuit platform to hybrid integrated optical WDM transceiver/receiver module," *Electron. Lett.*, vol. 31, pp. 1366–1367, 1995.

[7] K. Jinguji and M. Kawachi, "Synthesis of coherent two-port lattice-form optical delay-line circuit," *J. Lightwave Technol.*, vol. 13, pp. 73–82, 1995.

[8] K. Takiguchi, K. Jinguji, and Y. Ohmori, "Variable group-delay dispersion equaliser based on a lattice-form programmable optical filter," *Electron. Lett.*, vol. 31, pp. 1240–1241, 1995.

[9] M. Kawachi, "Silica waveguides on silicon and their application to integrated components," *Opt. Quantum Electron.*, vol. 22, pp. 391–416, 1990.

[10] Y. Yamada, A. Takagi, I. Ogawa, M. Kawachi, and M. Kobayashi, "Silica-based optical waveguide on terraced silicon substrate as hybrid integration platform," *Electron. Lett.*, vol. 29, pp. 444–445, 1993.

[11] T. Hashimoto, Y. Nakasuga, Y. Yamada, H. Terui, M. Yanagisawa, K. Moriwaki, T. Tohmori, Y. Suzuki, and M. Horiguchi, "Hybrid integration of a laser diode chip on a planar lightwave circuit platform by passive alignment method," *MOC'95 Tech. Dig.*, vol. D5, pp. 66–69, 1995.

[12] Y. Akahori, T. Ohyama, T. Hashimoto, and Y. Yamada, "Assembly and wiring technologies on PLC platforms for low-cost and high-speed applications," in *Proc. 47th ECTC'97*, 1997, pp. 632–637.

[13] Y. Yamada, S. Suzuki, K. Moriwaki, Y. Hibino, Y. Tohmori, Y. Akatsu, Y. Nakasuga, T. Hashimoto, H. Terui, M. Yanagisawa, Y. Inoue, Y. Akahori, and R. Nagase, "Application of planar lightwave circuit platform to hybrid integrated optical WDM transceiver/receiver module," *Electron. Lett.*, vol. 31, pp. 1366–1367, 1995.

[14] K. Kato, A. Kozen, M. Yuda, Y. Muramoto, K. Noguchi, Y. Akatsu, O. Nakajima, and J. Yoshida, "Low-cost low driving-voltage waveguide *p-i-n* photodiode for optical hybrid integration," in *Proc. OECC'96*, vol. 18D3-5, 1996.

[15] T. Tanaka, H. Takahashi, T. Hashimoto, Y. Yamada, and Y. Itaya, "Fabrication of hybrid integrated 4-wavelength laser composed of UV written waveguide grating and laser diodes," in *Proc. OECC'97*, vol. 10D3-3, 1997.

[16] H. Takahashi, T. Tanaka, Y. Akahori, T. Hashimoto, Y. Yamada, and Y. Itaya, "A 2.5 Gb/s, 4-channel multiwavelength light source composed of UV written waveguide gratings and laser diodes integrated on Si," in *Proc. ECOC'97*, 1997, pp. 3/355–3/358.

[17] A. Misawa, K. Sasayama, and T. Matsunaga, "Fast wavelength selection for four-channel wavelength division multiplexed 10 Gbit/s optical cells," *Electron. Lett.*, vol. 31, pp. 1763–1764, 1995.
[18] I. Ogawa, F. Ebisawa, N. Yoshimoto, K. Takiguchi, F. Hanawa, T. Hashimoto, A. Sugita, M. Yanagisawa, Y. Inoue, Y. Yamada, Y. Tohmori, S. Mino, T. Ito, K. Magari, Y. Kawaguchi, A. Himeno, and K. Kato, "Lossless hybrid integrated 8-ch optical wavelength selector module using PLC platform and PLC-PLC direct attachment techniques," in *Proc. OFC'98*, vol. PD4-1, 1998.
[19] Y. Akahori, T. Ohyama, M. Oguma, K. Kato, and Y. Yamada, "Hybrid integrated differential photoreceiver module for photonic packet switching systems using a planar lightwave circuit platform," *IEEE Photon. Technol. Lett.*, vol. 10, pp. 869–871, 1998.
[20] *Proc. Int. Conf. Integrated Optics and Communication*, 1977, p. 375.
[21] Y. Hida, Y. Hibino, H. Okazaki, and Y. Ohmori, "10 m long silica-based waveguide with a loss of 1.7 dB/m," in *Proc. IPR*, 1995. paper IThC6.
[22] Y. Hida, T. Fukumitsu, F. Hanawa, Y. Enomoto, S. Sumida, and N. Takato, "Highly compact silica-based PLC-type1×32 splitters using 127 μm-spacing output and 0.4%-Δ waveguides," *Electron. Lett.*, vol. 34, no. 1, pp. 75–76, 1998.
[23] Y. Hibino, F. Hanawa, H. Nakagome, N. Takato, T. Miya, and M. Yamaguchi, "High reliability silica-based PLC1×8 splitters on Si," *Electron. Lett.*, vol. 30, no. 8, pp. 640–641, 1994.
[24] Y. Hibino, F. Hanawa, N. Takato, H. Nakagome, Y. Inoue, T. Miya, and M. Yamaguchi, "Silica-based PLC splitters which satisfy reliability requirements for more than 5000 hours," in *OFC '94*, 1994, postdeadline paper PD-7.
[25] Y. Hibino, F. Hanawa, H. Nakagome, M. Ishii, and N. Takato, "High reliability optical splitters composed of silica-based planar lightwave circuits," *J. Lightwave Technol.*, vol. 13, pp. 1728–1735, 1995.
[26] H. Hanafusa, F. Hanawa, Y. Hibino, and T. Nozawa, "Reliability estimation for PLC-type optical splitters," *Electron. Lett.*, vol. 33, pp. 238–239, 1997.
[27] K. Jinguji, N. Takato, A. Sugita, and M. Kawachi, "Mach-Zehnder interferometer type optical waveguide coupler with wavelength-flattened coupling ratio," *Electron. Lett.*, vol. 26, no. 17, pp. 1326–1327, Aug. 1990.
[28] T. Miya, N. Takato, F. Janawa, Y. Ohmori, M. Yamaguchi, and N. Tomita, "Arrayed waveguide-type wavelength insensitive coupler for FTTH networks," in *Proc. OFC'92*, 1992, paper FA5.
[29] T. Oguchi, N. Takato, H. Hanafusa, N. Tomita, Y. Enomoto, and N. Nakao, "Design and fabrication of highly-dense optical components for in-service fiber testing and monitoring in subscriber loops," *IEICE Trans. Electron.*, vol. E80-C, no. 1, pp. 123–129, Jan. 1997.
[30] Q. Lai, M. Bachmann, and H. Melchior, "Low loss$1 \times n$ multimode interference couplers with homogeneous output power distributions realized in silica on Si material," *Electron. Lett.*, vol. 33, no. 20, pp. 1699–1700, 1997.
[31] H. Takahashi, S. Suzuki, K. Kato, and I. Nishi, "Arrayed waveguide grating for wavelength division multi/demultiplexer with nanometer resolution," *Electron. Lett.*, vol. 26, pp. 87–88, 1990.
[32] M. K. Smit, "New focusing and dispersive planar component based on an optical phased array," *Electron. Lett.*, vol. 24, pp. 385–386, 1988.
[33] C. Dragone, C. A. Edwards, and R. C. Kistler, "Integrated optics$N \times N$ multiplexer on silicon," *IEEE Photon. Technol. Lett.*, vol. 3, pp. 896–899, 1991.
[34] H. Takahashi, K. Oda, H. Toba, and Y. Inoue, "Transmission characteristics of arrayed-waveguide$N \times N$ wavelength multiplexer," *J. Lightwave Technol.*, vol. 13, pp. 447–455, 1995.
[35] Y. Inoue, H. Takahashi, S. Ando, T. Sawada, A. Himeno, and M. Kawachi, "Elimination of polarization sensitivity in silica-based wavelength division multiplexer using a polyimide half waveplate," *J. Lightwave Technol.*, vol. 15, pp. 1947–1957, 1997.
[36] S. Suzuki, S. Sumida, Y. Inoue, M. Ishii, and Y. Ohmori, "Polarization-insensitive arrayed-waveguide grating using dopant-rich silica based glass with thermal expansion adjusted to Si substrate," *Electron. Lett.*, vol. 33, no. 13, pp. 1173–1174, 1997.
[37] K. Okamoto, K. Shuto, H. Takahashi, and Y. Ohmori, "Fabrication of 128-channel arrayed-waveguide grating multiplexer with 25 GHz spacing," *Electron. Lett.*, vol. 32, pp. 1474–1475, 1996.
[38] H. Uetsuka, K. Akiba, K. Morosawa, H. Okano, S. Takasugi, and K. Inaba, "Demultiplexer with arrayed waveguide grating," *IEICE Trans. Electron.*, vol. E80-C, no. 5, May 1997.
[39] K. Okamoto *et al.*, "Arrayed waveguide grating multiplexer with flat spectral response," *Opt. Lett.*, vol. 20, pp. 43–45, 1995.
[40] M. R. Amersfoort *et al.*, "Passband broadening of integrated arrayed waveguide filters using multimode interference couplers," *Electron. Lett.*, vol. 32, pp. 449–451, 1996.
[41] D. Trouchet *et al.*, "Passband flattening of PHASAR WDM using input and output star couplers designed with two focal points," in *Proc. OFC'97*, Dallas, Texas, 1997.
[42] G. H. B. Thompson *et al.*, "An original low-loss and pass-band flattened SiO_2 on Si planar wavelength demultiplexer," in *OFC'98*, 1998, pp. 77–78.
[43] K. Okamoto and A. Sugita, "Flat spectral response arrayed-waveguide grating multiplexer with parabolic waveguide horns," *Electron. Lett.*, vol. 32, pp. 1661–1662, 1996.
[44] Y. Inoue, A. Kaneko, F. Hanawa, H. Takahashi, K. Hattori, and S. Sumida, "Athermal silica-based arrayed-waveguide grating multiplexer," *Electron. Lett.*, vol. 33, pp. 1945–1946, 1997.
[45] M. Okuno, N. Takato, T. Kitoh, and A. Sugita, "Silica-based thermooptic switches," *NTT Rev.*, vol. 7, pp. 57–63, 1995.
[46] T. Kominato, A. Himeno, M. Ishii, T. Goh, K. Hattori, F. Hanawa, and K. Kato, "Silica-based optical switch with a single-facet array fiber connection," in *Proc. CLEO Passific Rim*, Makuhari, Japan, 1997. paper FH2.
[47] T. Goh, A. Himeno, M. Okuno, H. Takahashi, and K. Hattori, "High extinction ratio and low loss silica-based8×8 thermooptic matrix switch," *IEEE Photon. Technol. Lett.*, vol. 10, pp. 358–360, 1998.
[48] T. Goh, M. Yasu, K. Hattori, A. Himeno, and Y. Ohmori, "Low loss and high extinction ratio silica-based strictly nonblocking16×16 thermooptic matrix switch," *IEEE Photon. Technol. Lett.*, vol. 10, pp. 810–812, 1998.
[49] T. Nishi, T. Yamamoto, and S. Kuroyanagi, "A polarization-controlled free-space photonic switch based on a PI-LOSS switch," *IEEE Photon. Technol. Lett.*, vol. 5, pp. 1104–1106, 1993.
[50] R. Nagase, A. Himeno, M. Okuno, K. Kato, K. Yukimatsu, and M. Kawachi, "Silica-based8×8 optical matrix switch module with hybrid integrated driving circuits and its system application," *J. Lightwave Technol.*, vol. 12, pp. 1631–1639, 1994.
[51] W. Hunziker and H. Melchior, "Low power compact2×2 thermooptical silica on silicon waveguide switch with fast response," *IEEE Photon. Technol. Lett.*, vol. 10, no. 5, pp. 681–683, 1998.
[52] K. Okamoto, M. Okuno, A. Himeno, and Y. Ohmori, "16-ch optical add/drop multiplexer consisting of arrayed waveguide gratings and double-gate switches," *Electron. Lett.*, vol. 32, pp. 1471–1472, 1996.
[53] C. K. Madsen *et al.*, "A multi-port add/drop router using UV-induced gratings in planar waveguides," in *Proc. OFC'99*, 1999, pp. 104–106.
[54] H. Li *et al.*, "8-wavelength photonic integrated2×2 WDM cross-connect switch using$2 \times N$ phased-array waveguide grating (PAWG) multi-demultiplexers," *Electron. Lett.*, pp. 592–594, 1997.
[55] B. J. Offrein, G. L. Bona, and F. Horst *et al.*, "Wavelength tunable optical add after drop filter with flat passband for WDM networks," *IEEE Photon. Technol. Lett.*, vol. 11, no. 2, pp. 239–241, 1999.
[56] K. Takiguchi, S. Kawanishi, H. Takara, A. Himeno, and K. Hattori, "Dispersion slope equalizer for dispersion shifted fiber using a lattice-form programmable optical filter on a planar lightwave circuit," *J. Lightwave Technol.*, vol. 16, pp. 1647–1656, Sept. 1998.

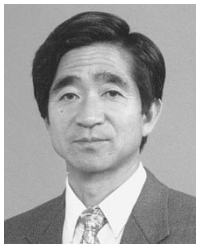

Tetsuo Miya (M'84) was born in Niigata, Japan, on February 9, 1950. He received the M.S. degree in physics and the doctor degree of engineering from Tohoku University, Sendai, Japan, in 1973 and 1975, respectively.

In 1975, he joined Ibaraki Electrical Communication Laboratory, Nippon Telegraph and Telephone Corporation (NTT), Japan. His main activities include research on measurement method of refractive index profiles in optical fibers and research on optical single-mode fiber fabrication by two methods: MCVD and vapor-phase axial deposition. He has successfully realized the ultra-low-loss single-mode fiber with a loss of 0.2 dB/km in 1979. After several years in administrative staff of the laboratories, he has been engaged in research on planar lightwave circuits (PLC's). He started a new business concerning PLC devices and Pr-doped optical fiber amplifier in NTT Electronics (NEL), one of the subsidiaries of NTT, in 1995. He is now Executive Manager of the Hyper-Photonic Component Laboratory, NTT Photonics Laboratories.

Dr. Miya is a member of the Institute of Electronics, Information and Communication Engineers of Japan and the Japan Society of Applied Physics. His paper published in *Electronics Letters* in 1979 was nominated by the Institute for Science Information, PA, as one of the most cited papers in 1985.